**Journal of Animal & Plant Sciences, 35(6): 2025, Page: 1691-1701**
**ISSN (print): 1018-7081; ISSN (online): 2309-8694**
https://doi.org/10.36899/JAPS.2025.6.0142

# MECHANISM OF HUOXUE HUAYU DECOCTION PROMOTING TIBIAL FRACTURE HEALING IN RATS VIA NOTCH1/PPARΓ/CD36 SIGNALING PATHWAY

F. Zhao and M. Wang*

Department of Traditional Chinese Medicine, Xidian Group Hospital, Xi'an, 710086, Shaanxi, China.
*Corresponding author: Mian Wang: Email: wangmian0086@163.com

## ABSTRACT

Tibial fractures are a common type of traumatic injury, typically treated through surgical reduction and fixation; however, the healing outcomes are often suboptimal. This work aimed to investigate the mechanism of Huoxue Huayu Decoction (HXHYD, a traditional Chinese herbal formula composed of *Bupleuri Radix*, *Paeoniae Radix Alba*, and *Leonuri Herba* known for promoting blood circulation and resolving stasis) promoting tibial fracture healing in rats via Notch1/PPARγ/CD36 pathway. Forty-eight male Sprague-Dawley rats of clean grade were randomly allocated into a control group (sham surgery, 10 mL/kg/d saline gavage, n=12), a model group (fracture model, 10 mL/kg/d saline gavage, n=12), a positive group (fracture model, 0.27 g/kg/d Xianling Gubao capsule gavage (standardized extract equivalent to human dose of 3 g/d, calculated by body surface area, n=12), and a HXHYD group (fracture model, 13.45 mL/kg/d HXHYD gavage, n=12). Rats in each group were administered gavage once daily for 28 consecutive days. X-ray imaging outcomes and Lane-Sandhu scores were employed to assess tibial fracture healing. Enzyme-linked immunosorbent assay (ELISA) measured serum inflammatory cytokine levels and bone formation markers. Tibial tissue from rats was collected to measure biomechanical parameters. Western blot analysis quantified bone-regulatory factors' expression. Relative to control group, model group showed a reduced Lane-Sandhu score, elevated serum TNF-α, IL-1β, IL-6, and bone formation markers ALP, BGP, and IGF-1, and a decrease in tibial maximum load, elastic load, and maximum deflection. Additionally, tibial BMP-2, RUNX2, VEGF, Notch1, and CD36 protein levels were increased, while tibial PPARγ protein expression was decreased ($P$<0.05). HXHYD group showed the most prominent improvements, including a 45% increase in Lane-Sandhu score, 30% reduction in TNF-α levels, and 50% elevation in BMP-2 expression versus model group ($P$<0.05). HXHYD also enhanced maximum tibial load (25.3±2.1 N *vs.* 18.5±1.8 N in model group) and suppressed PPARγ expression by 40%, while upregulating Notch1 and CD36 ($P$<0.05). Relative to positive group, HXHYD group showed more pronounced improvements in all indicators ($P$<0.05). HXHYD promotes tibial fracture healing by alleviating inflammation, enhancing osteogenesis, and modulating Notch1/PPARγ/CD36 pathway. Hence, HXHYD can serve as a complementary therapy to surgery, optimizing the bone repair microenvironment and accelerating functional recovery.

**Keywords:** tibial fracture; Huoxue Huayu Decoction; inflammation; biomechanics; Notch1/PPARγ/CD36 pathway



Published first online October 08, 2025 Published final November 30, 2025

## INTRODUCTION

Tibial fractures, including both tibial shaft and tibial plateau fractures, are common in knee joint injuries and can lead to restricted mobility, significantly affecting patients' quality of life (Wood *et al*., 2024; Pai and Kumar, 2023). Currently, surgical treatment is the primary approach for managing these fractures. Adequate reduction and fixation provide ideal conditions for early fracture healing; however, delayed healing and non-union rates remain as high as 5–10% (Cruz *et al*., 2024). Therefore, identifying more effective and safer treatment options is crucial for enhancing the quality of life and prognosis of patients with tibial fractures.

Compared to certain chemical drugs, natural plants generally demonstrate higher safety in fracture treatment (*e.g.,* lower incidence of allergic reactions and hepatic or renal toxicity); however, their long-term safety requires systematic evaluation (Yong *et al.,* 2021). The formulation of Huoxue Huayu Decoction (HXHYD) includes Chaihu (*Bupleuri Radix*), Baishao (*Paeoniae Radix Alba*), Yimucao (*Leonuri Herba*), Jixueteng (*Spatholobi Caulis*), Danggui (*Angelicae Sinensis Radix*), Danshen (*Salviae Miltiorrhizae Radix*), Chishao (*Paeoniae Radix Rubra*), Zelan (*Lycopi Herba*), Huainiu Xi (*Achyranthis Bidentatae Radix*), Liujinu (*Artemisia anomala*), and Sumu (*Sappan Wood*). The formula is centered on promoting blood circulation and resolving blood stasis. Through mechanisms including peripheral

vasodilation, improved blood flow, and reduced blood viscosity, it enhances local microcirculation (Zhang *et al.,* 2023).

Multiple meta-analyses indicated that HXHYD exhibits potential therapeutic effects across various diseases. Hou *et al.* (2022) confirmed that it can reduce the risk of restenosis in patients after percutaneous coronary intervention. Zheng *et al.* (2020) found that HXHYD injection effectively controls blood pressure and renal function parameters in patients with hypertensive nephropathy (Hou *et al.,* 2022; Zheng *et al.,* 2020). Basic research noted that HXHYD can repair neurological function in rats with severe traumatic brain injury by activating Wnt/β-catenin signaling (Wang *et al.,* 2020; Zheng *et al.,* 2014).

Although HXHYD has demonstrated significant effects in anti-inflammatory responses, vascular regeneration, and tissue repair, its mechanism of action in fracture healing remains unclear. Hence, this work established a tibial fracture rat model and investigated the molecular mechanism by which HXHYD gavage treatment influences fracture healing progression through Notch1/PPARγ/CD36 pathway. The aim was to provide reference data for understanding the potential mechanisms by which HXHYD promotes fracture healing.

## MATERIALS AND METHODS

**Preparation of HXHYD:** The composition of the formula includes: Chaihu (10 g), Baishao (15 g), Yimucao (15 g), Jixueteng (15 g), Danggui (15 g), Danshen (15 g), Chishao (12 g), Zelan (12 g), Huainiu Xi (12 g), Liujinu (12 g), and Sumu (12 g). The herbal pieces of HXHYD were placed in a decoction pot and soaked in drinking water for 30 minutes (enough to cover the herbs with water). The mixture was then brought to a boil over high heat, and the heat was lowered to a simmer and continued until approximately 150 mL of the decoction remained. The concentration of the decoction was calculated using the equation: herb weight (g) / decoction volume (mL), resulting in a concentration of approximately 0.97 g/mL.

**Establishment of tibial fracture model:** The study employed 48 male Sprague-Dawley (SD) rats (8 weeks old, weighing 260–300 g), sourced from Beijing Vital River Laboratory Animal Technology Co., Ltd. (China). Housing conditions included an SPF facility with controlled environmental parameters (22–24°C, 50–60% humidity, 12-hour light/dark cycle) and ad libitum access to sterile rodent feed and autoclaved water. The research experiments conducted with animals were approved by the Ethical Committee of Xidian Group Hospital and responsible authorities of research organization(s) following all guidelines, regulations, legal, and ethical standards as required for animals.

Thirty-six rats were randomly selected to construct the tibial fracture model, while the remaining twelve rats served as control group. After one week of acclimatization, the rats were fasted for 12 hours before the surgery and were anesthetized with an intraperitoneal injection of 3% sodium pentobarbital (Sigma-Aldrich, USA) at a dose of 30 mg/kg. The right hindlimb of the rat was fixed in a sterile laminar flow cabinet, and the skin was shaved and disinfected. A 1.5 cm incision was made at the 1/3 region of the lower leg, followed by sequential dissection of the skin, subcutaneous tissue, fascia, and tibialis anterior muscle to expose the tibial tuberosity. A transverse osteotomy was performed 1 cm below the tibial tuberosity, and a 1 mm Kirschner wire (Shijiazhuang Dabang Medical Instrument Factory, China) was inserted through the medullary cavity of the distal bone fragment, piercing both the cortical bone and skin. The fracture was realigned, and satisfactory reduction was achieved. The Kirschner wire was inserted in reverse and fixed in place. The wound was irrigated with saline, hemostasis was achieved, and the incision was closed with sutures. Routine disinfection was performed to prevent infection. Fracture status was confirmed by anteroposterior high-resolution X-ray images (Beijing Kubot International Technology Co., Ltd., China), with successful fracture model establishment defined by either a transverse or short oblique fracture pattern. The right hindlimb was then immobilized with polymer resin bandages, and the rats were placed in a warming chamber to recover.

**Animal grouping and intervention:** Forty-eight male SD rats (8 weeks old, weighing 260–300 g) were weighed, and their baseline data were recorded prior to the experiment. Stratified block randomization was employed to ensure balanced weight distribution across groups. The rats were sorted by weight in ascending order and divided into twelve blocks (four rats per block). A random sequence for each block of four rats was generated using a random number generator (Random.org) and subsequently assigned to control, model, positive, and HXHYD groups. One-way analysis of variance (ANOVA) confirmed negligible differences in body weight among these groups ($P > 0.05$). Ultimately, each group included twelve rats. During the experiment, if any rat died due to surgical complications or infection, it was excluded based on predefined criteria and replaced with an additional rat from the backup pool, following the same randomization method, ensuring a constant sample size in each group. The treatment procedures for the rats in each group were as follows:

Control group received sham surgery. The skin of the right hindlimb was incised, the tibia was exposed, and the wound was directly sutured and disinfected.

Subsequently, the rats were gavaged with 10 mL/kg/day of 0.9% sodium chloride solution.

For model group, after the tibial fracture model was successfully established, the dosage of 0.9% sodium chloride solution was calculated according to the relevant standards outlined in the *Pharmacological Experimental Methodology of Traditional Chinese Medicine* (Shang *et al*., 2023), and the rats were gavaged with 10 mL/kg/day of 0.9% sodium chloride solution.

For positive group, after successful establishment of the tibial fracture model, rats were administered 0.27 g/kg/day of Xianling Gubao capsules (Guizhou Tongjitang Pharmaceutical Co., Ltd., China) by gavage. The dose for human is 3 g/day, which, based on the body surface area conversion formula, corresponds to 0.27 g/kg for rats. The 0.27 g of drug powder was dissolved in 10 mL of 0.9% sodium chloride solution and administered via gavage. Xianling Gubao is a commonly used clinical Chinese herbal compound, with main ingredients including Epimedium, Dipsacus, and Psoralea, and has been shown to promote osteoblastic differentiation through the activation of the BMP/Smad pathway (Zhou *et al.,* 2023). This study selected Xianling Gubao as a positive control to compare the efficacy differences between HXHYD and known bone-healing drugs, thus verifying the specific regulatory role of the Notch1/PPARγ/CD36 pathway.

For HXHYD group, after the tibial fracture model was successfully established, the rats were gavaged with 13.45 mL/kg/day of HXHYD. The dose for human is 145 g/day, and the dosage for rat was calculated as 13.05 g/kg based on the body surface area conversion equation. Therefore, the gavage dosage for the rats = herbal dose / decoction concentration ≈ 13.45 mL/kg.

Each group of rats was gavaged once daily for 28 consecutive days. During the experiment, if any rat died due to surgical complications or infection (a total of two rats, one from model group and one from HXHYD group), it was excluded based on predefined criteria and replaced with an additional rat from the backup pool, following the same randomization method, thus ensuring that the final sample size for each group remained twelve rats.

**Tibial fracture healing observation:** After the intervention, tibial fracture healing was assessed using anteroposterior X-ray imaging to observe callus formation and fracture healing. The Lane-Sandhu scoring system was employed to evaluate healing based on three criteria: i) Bone formation, with scores ranging from 0 (no bone formation) to 4 (75-100% of the defect occupied by bone); ii) Bone union, where 0 points indicate a clear fracture line, 2 points represent partial presence of the fracture line, and 4 points indicate complete disappearance of the fracture line; iii) Bone remodeling, with 0 points for no remodeling, 2 points for medullary cavity formation, and 4 points for cortical bone remodeling. A higher Lane-Sandhu score corresponds to better fracture healing.

**Detection of serum inflammatory and bone formation cytokine levels:** After the intervention, rats were anesthetized by intraperitoneal injection of 30 mg/kg 3% pentobarbital sodium. Serum in blood samples collected from abdominal aorta was separated by centrifugation at 3000 rpm for 10 minutes. Serum levels of inflammatory cytokines, tumor necrosis factor (TNF)-α, interleukin (IL)-1β, and IL-6, as well as bone formation cytokines, including alkaline phosphatase (ALP), bone gla protein (BGP), and insulin-like growth factor-1 (IGF-1), were measured employing enzyme-linked immunosorbent assay (ELISA) kits (Shanghai Beyotime Biotechnology Co., Ltd., China). All procedures were strictly performed regarding the manufacturer's instructions.

**Detection of tibial biomechanical parameters:** After blood collection, rats were euthanized by cervical dislocation under anesthesia induced by intraperitoneal injection of 30 mg/kg 3% pentobarbital sodium. The right tibia was then excised, with soft tissue and joint protrusions removed without damaging the callus, and the bone surface was smoothed before removing the Kirschner wire. The tibia was placed on the support of a universal material testing machine (Shandong Wancheng Testing Machine Co., Ltd., China), and a compressive load was applied at a rate of 1 mm/s until the tibia fractured. The maximum load, elastic load, and maximum deflection, as well as other biomechanical parameters, were obtained from the automatically generated load-deformation curve.

**Western blotting analysis:** A 100 mg sample of tibial tissue from the right hind limb of the rats was homogenized in pre-chilled radioimmunoprecipitation assay lysis buffer (containing protease inhibitors, Sigma-Aldrich, USA) and incubated on ice for 30 minutes. The mixture was then centrifuged at 12,000 × g for 15 minutes at 4°C, and the supernatant was collected to remove cellular debris. Bicinchoninic acid assay (Pierce™ BCA Protein Assay Kit, Thermo Fisher Scientific, USA) determined total protein concentration. The samples were then adjusted to a uniform concentration (50 μg/well), aliquoted, and stored at -80°C for long-term use, avoiding repeated freeze-thaw cycles.

Fifty micrograms of protein samples were mixed with 5× Loading Buffer and denatured at 95°C for 5 minutes. The mixture was loaded onto a 12% sodium dodecyl sulfate-polyacrylamide gel, and electrophoresis was carried out at a constant voltage of 80 V until the concentrated and separating gels interfaced. The voltage was then increased to 120 V, and electrophoresis continued until the bromophenol blue marker reached the bottom of the gel. Wet transfer was performed using the

Bio-Rad Trans-Blot® system, transferring proteins to a polyvinylidene fluoride membrane at a constant current of 200 mA, with transfer time adjusted regarding the protein molecular weight (BMP-2: 90 minutes; RUNX2: 60 minutes). The membrane was then blocked with 5% skim milk (prepared in Tris buffered saline Tween (TBST)) at 25°C for 1 hour. Primary antibodies were applied (Abcam, UK), and the membrane was incubated overnight at 4°C: bone morphogenetic protein-2 (BMP-2, 1:1000); Runt-related transcription factor 2 (RUNX2, 1:1000); vascular endothelial growth factor (VEGF, 1:800); Notch1 (1:1200); peroxisome proliferator-activated receptor γ (PPARγ, 1:1000); cluster of differentiation 36 (CD36, 1:800); β-actin (1:2000, internal control). After washing with TBST thrice (10 minutes each), a horseradish peroxidase (HRP)-conjugated goat anti-rabbit secondary antibody (1:5000, Abcam, UK) was applied and incubated at 25°C for 1 hour. The enhanced chemiluminescence substrate (Shanghai Biotntian Biotechnology Co., Ltd., China) was utilized for detection, and images were captured using *Image Lab 6.0* (Bio-Rad, USA). β-actin served as internal reference, and target protein relative expression level was calculated as the ratio of the target protein's grayscale value to internal reference grayscale value. Each group of samples was independently repeated thrice, with the fluctuation in β-actin expression across groups being less than 10% (CV value), meeting the stability criteria for the internal reference.

**Statistical analysis:** All data were denoted as mean ± standard deviation ($\bar{x}$±s). Data normality was verified using the Shapiro-Wilk test, while variance homogeneity was examined via the Levene test. For data satisfying both assumptions, intergroup comparisons were performed using one-way ANOVA, and intergroup differences were further analyzed using the LSD-t test. For multiple comparisons (*e.g.,* inflammatory factors, osteogenic markers, and multiple pathway proteins), Bonferroni correction was applied to adjust the significance level (adjusted $P<0.0167$). For non-normally distributed data, the Kruskal-Wallis test was applied. All analyses were conducted in SPSS 23.0, with statistical significance set at $P<0.05$.

## RESULTS

**Impact of HXHYD on fracture healing in tibial fracture rats:** In Figure 1A, the fracture line in the model group was relatively clear with no callus formation, while the fracture lines in positive group and HXHYD group were blurred and accompanied by callus formation. The Lane-Sandhu scoring system evaluates fracture healing based on three dimensions (total score range: 0–12 points): bone formation (0–4 points): 0 points (no bone formation), 4 points (75–100% of the defect area filled with bone); bone healing (0–4 points): 0 points (clear fracture line), 4 points (complete disappearance of the fracture line), bone remodeling (0–4 points): 0 points (no remodeling), 4 points (complete cortical bone remodeling). A higher score indicates a better degree of fracture healing. In Figure 1B, control group had a score of 9.8 ± 0.5, while model group was markedly reduced to 4.2 ± 1.1 ($P<0.001$). The scores of positive group and HXHYD group were 7.6 ± 0.8 and 8.9 ± 0.7, respectively, which greatly surpassed model group ($P<0.05$). Additionally, HXHYD group showed a 17% improvement versus positive group ($P<0.05$), indicating that HXHYD can accelerate bone healing and remodeling ($P<0.05$, Cohen's d=1.5).

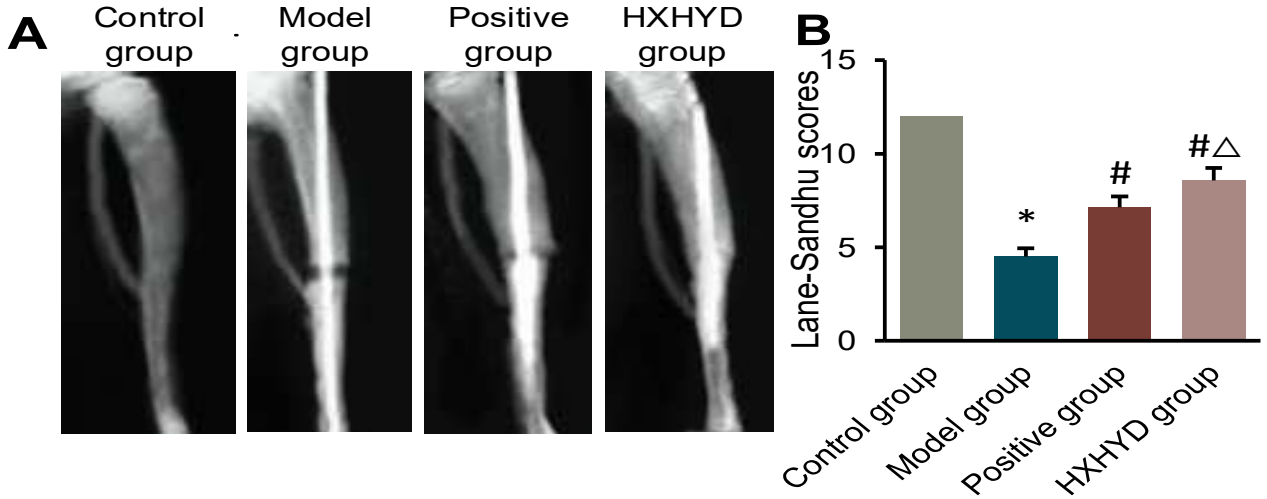


**Fig. 1. Observation of fracture healing in rats of different groups. A: anteroposterior X-ray images of the tibia; B: Lane-Sandhu score. *$P<0.05$ *vs.* control group; #$P<0.05$ *vs,* model group; Δ$P<0.05$ *vs.* positive group (in Figs. 1-6).**

**Influence of HXHYD on inflammatory response in tibial fracture rats:** In Figure 2A–2C, serum TNF-α, IL-1β, and IL-6 in model group markedly surpassed those in control group ($P$<0.05). These inflammatory cytokine levels in positive group and HXHYD group were markedly inferior to those in model group ($P$<0.05), and the levels in HXHYD group were notably inferior to those in positive group ($P$<0.05). Serum TNF-α in HXHYD group (15.2 ± 2.1 pg/mL) was reduced by 53% versus model group (32.5 ± 3.4 pg/mL) ($P$<0.001) and was notably inferior to that in positive group (20.8 ± 2.6 pg/mL) (Figure 2A). Hence, HXHYD demonstrated superior anti-inflammatory activity versus positive group by substantially lowering serum TNF-α levels. This effect may involve specific regulation of TNF-α synthesis, secretion, or pathways.

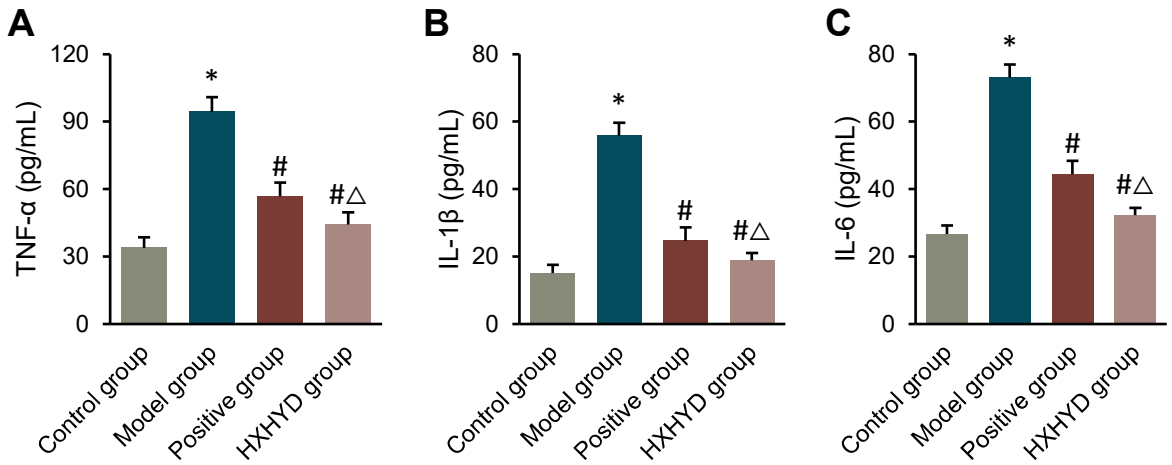


**Fig. 2. Comparison of serum inflammatory cytokine levels of different groups.**

**Effect of HXHYD on bone formation in tibial fracture rats:** In Figure 3A–3C, serum ALP, BGP, and IGF-1 levels in model group were drastically superior to those in control group ($P$<0.05). These bone formation cytokine levels in positive group and HXHYD group were greatly superior to those in model group ($P$<0.05), and these cytokine levels in HXHYD group were notably superior to those in positive group ($P$<0.05).

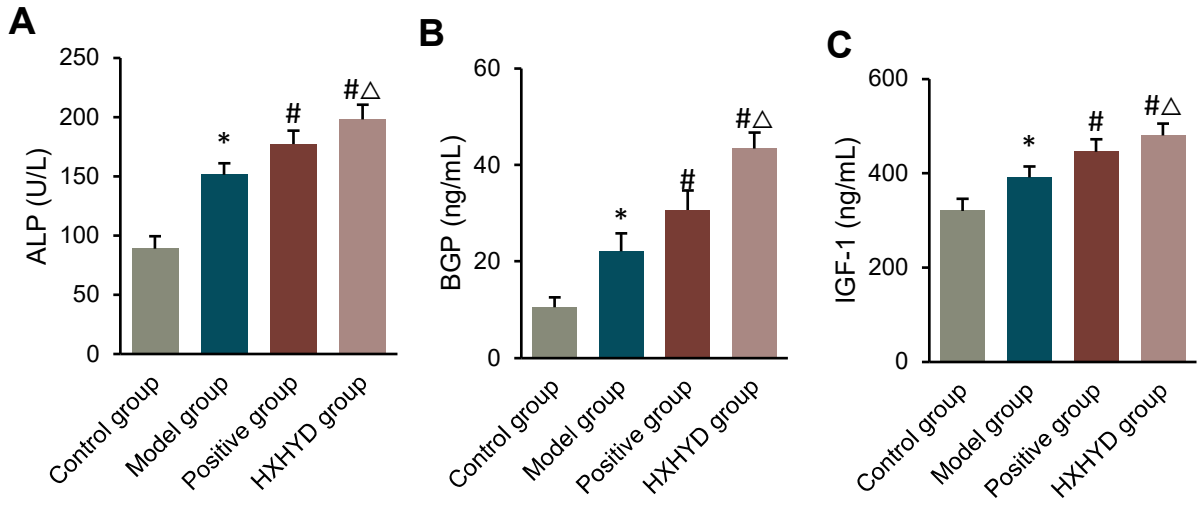


**Fig. 3. Comparison of serum bone formation factor levels of different groups.**

**Impact of HXHYD on bone biomechanical properties in tibial fracture rats:** In Figure 4A–4C, the tibial biomechanical parameters, including maximum load, elastic load, and maximum deflection, in model group were dramatically inferior to those in control group ($P$<0.05). The tibial biomechanical parameters in positive group and HXHYD group were drastically superior to those in model group ($P$<0.05), and the tibial

biomechanical parameters in HXHYD group were substantially superior to those in positive group ($P$<0.05).

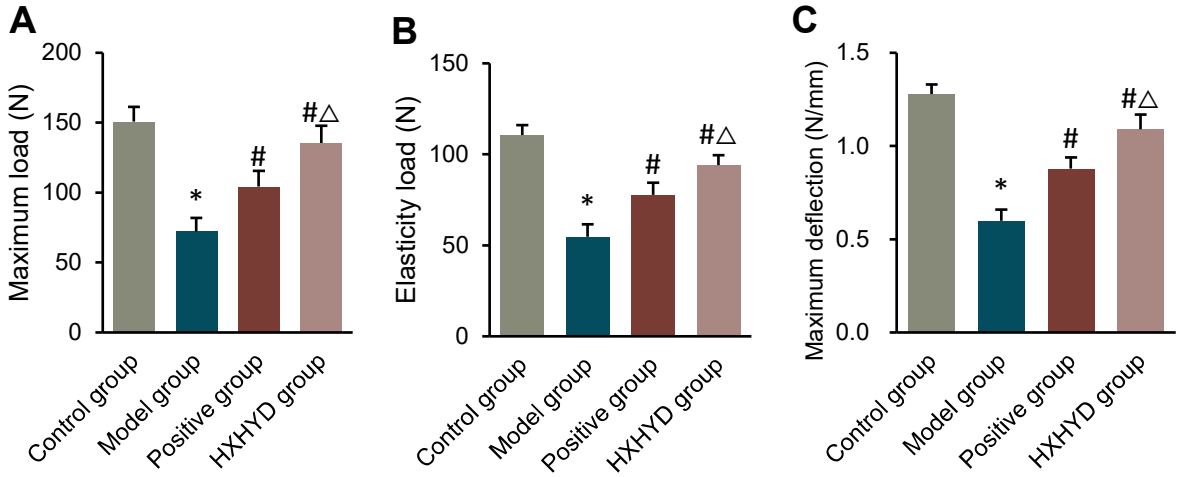


**Fig. 4. Comparison of tibial biomechanical parameters of different groups.**

**Impact of HXHYD on BMP-2, RUNX2, and VEGF protein relative expression in the tibia of tibial fracture rats:** In Figure 5A–5D, BMP-2, RUNX2, and VEGF protein relative levels in the tibia of rats in model group greatly surpassed those in control group ($P$<0.05). These protein relative levels in positive group and HXHYD group substantially surpassed those in model group ($P$<0.05), and these protein relative levels in HXHYD group notably surpassed those in positive group ($P$<0.05).

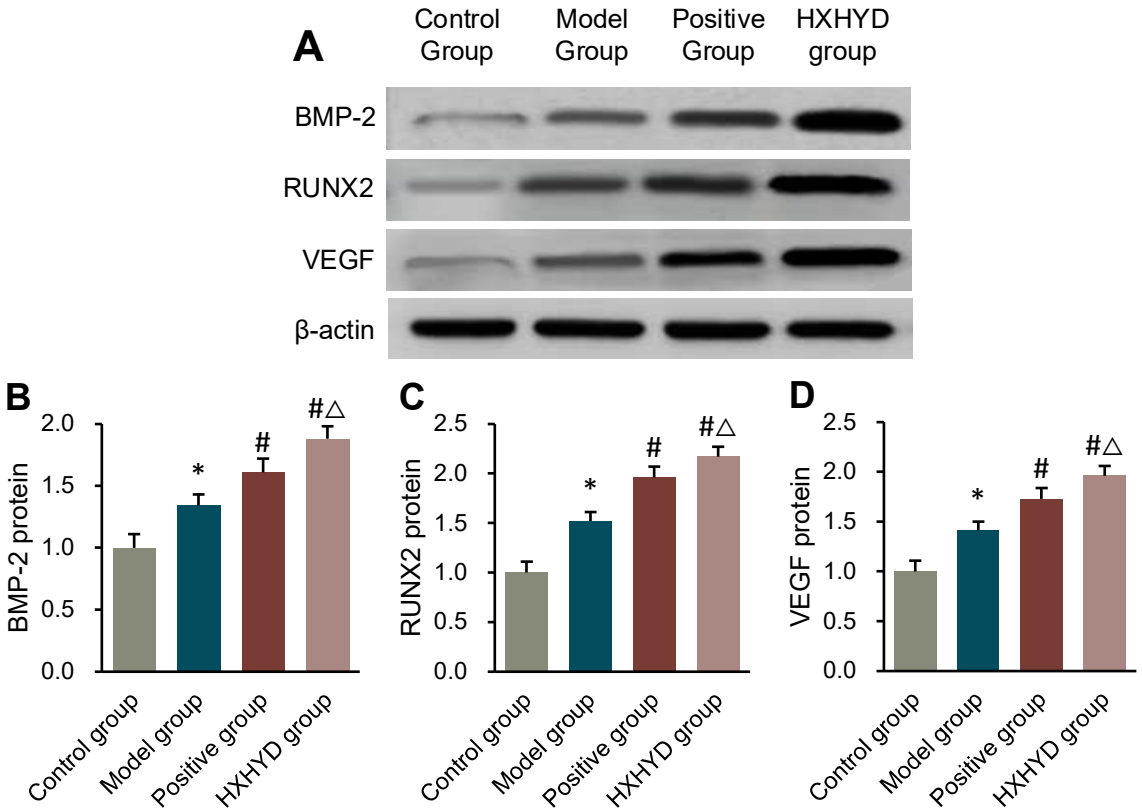


**Fig. 5. Comparison of BMP-2, RUNX2, and VEGF protein relative expression in the tibia of rats of different groups. A: Western blotting results; B: BMP-2 protein; C: RUNX2 protein; D: VEGF protein.**

**Influence of HXHYD on relative expression of tibial Notch1/PPARγ/CD36 pathway proteins in rats with tibial fractures:** Western blot results showed that BMP-2 (2.1 ± 0.3), RUNX2 (1.8 ± 0.2), and VEGF (2.4 ± 0.4) relative protein levels in HXHYD group were markedly surpassed those in other groups ($P$<0.05). Additionally, Notch1 (1.9 ± 0.2) (Figure 6B) and CD36 (2.2 ± 0.3) (Figure 6D) were upregulated, while PPARγ (0.6 ± 0.1) (Figure 6C) was downregulated, indicating that HXHYD promotes bone regeneration and angiogenesis through Notch1/PPARγ/CD36 pathway.

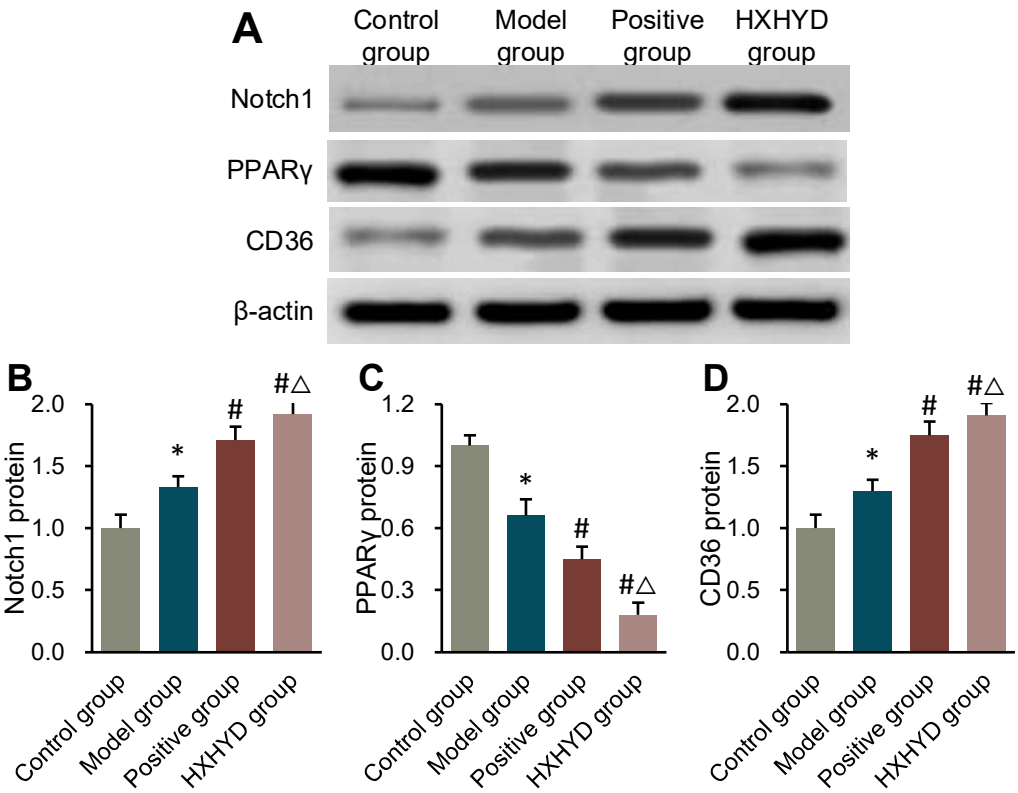


**Fig.6. Comparison of tibial Notch1/PPARγ/CD36 pathway protein relative expression in rats of different groups. A: Western blot results; B: Notch1 protein; C: PPARγ protein; D: CD36 protein.**

## DISCUSSION

To identify potential therapeutic agents for early fracture healing, this work established a rat model of tibial fracture and evaluated the mechanism of action of HXHYD on fracture healing. It was observed that after modeling, the tibial fracture line in the rats was clear, and the Lane-Sandhu score was reduced, indicating the successful establishment of the tibial fracture model. Subsequently, it was found that after oral administration of HXHYD, the fracture line in the model rats became blurred, and bone callus formation was observed, with a significant increase in the Lane-Sandhu score. Ling (2024) evaluated the effects of HXHYD on late-stage limb swelling and motor function in bone injury and found that the decoction effectively alleviated limb swelling, promoted motor function recovery, and reduced the incidence of adverse reactions (Ling, 2024). This suggests that HXHYD has potential therapeutic effects on promoting tibial fracture healing, although its underlying mechanism remains to be further explored. This study found that HXHYD significantly upregulated Notch1 protein expression (1.9-fold higher than the model group), which is consistent with the critical role of the Notch signaling in regulating osteogenic differentiation of mesenchymal stem cells (MSCs). Novak *et al.* (2020) confirmed that Notch1 activation can promote Runx2 transcription by inhibiting Hes1 protein, thereby driving MSCs to differentiate into osteoblasts while suppressing the expression of adipogenesis-related gene PPARγ (Novak *et al.,* 2020). This mechanism aligns closely with the findings of this study: in the HXHYD group, PPARγ expression was downregulated by 45%, while Runx2 expression increased 1.8-fold, suggesting that HXHYD may coordinate the balance between osteogenesis and inhibition of adipogenic differentiation via the Notch1-Runx2 axis. Wang *et al.* (2024) found that Notch1 overexpression enhances the angiogenic capacity of bone microvascular endothelial cells, further supporting the

notion that HXHYD promotes blood supply reconstruction at the fracture site through the Notch1/VEGF pathway (Wang *et al.,* 2024). During the fracture healing process, bone regeneration is regulated by cytokines, which interact with the tissues in the repair microenvironment (Muwanga *et al*., 2022). The increased activity of inflammatory cytokines can inhibit osteoblast differentiation to some extent and hinder bone healing (Zhang *et al*., 2022; Shimo *et al*., 2020; Coates *et al*., 2021). It was found that serum TNF-α, IL-1β, and IL-6 in tibial fracture rats were drastically elevated, while oral administration of HXHYD notably reduced these inflammatory cytokines in model rats' serum. Zhang *et al.* analyzed the use of HXHYD combined with ibuprofen in treating ankle fracture surgery patients and found that it effectively reduced postoperative TNF-α and IL-6, improved isokinetic muscle strength and ankle joint function, and accelerated fracture healing (Zhang *et al*., 2024). This suggests that HXHYD may modulate the osteoblastic differentiation process and influence fracture healing by inhibiting the release of pro-inflammatory cytokines TNF-α, IL-1β, and IL-6 following fracture. BGP reflects osteoblast activity, while ALP is essential for bone mineralization, and both are indicators of osteoblast activity during the fracture healing process. Elevated levels of BGP and ALP can accelerate fracture healing (Lin *et al*., 2024; Schumm *et al*., 2023). IGF-1, the most abundant growth factor in bone cells, is synthesized under the mediation of growth hormone and plays a vital role in osteoblast function (Costanzo *et al*., 2024). It was found that serum ALP, BGP, and IGF-1 were notably elevated in tibial fracture rats, and these levels were even more pronounced after oral administration of HXHYD. Following fracture, the body accelerates calcium-phosphate metabolism, promotes osteoblast synthesis, and releases more growth hormones to stimulate fracture repair and regeneration, resulting in elevated serum levels of ALP, BGP, and IGF-1 (Park *et al*., 2020). HXHYD further stimulates the synthesis and release of ALP, BGP, and IGF-1, thereby enhancing the activity of skeletal repair and regeneration at the fracture site, which is beneficial for the fracture healing process.

Bone biomechanics is a comprehensive representation of bone strength, structure, and mass, and a decrease in its performance is one of the key factors leading to fractures (Sabaté-Brescó *et al*., 2021). It was found that oral administration of HXHYD greatly increased the maximum load, elastic load, and maximum deflection of the tibia in rats with tibial fractures. This suggests that HXHYD can enhance the tibia's ability to withstand external forces and resist fractures. BMPs are multifunctional polypeptides in the TGF-β superfamily, whose primary function is promoting osteoblast differentiation and collagen synthesis and stimulating new bone formation through endochondral ossification. An increase in BMP-2 expression promotes the differentiation of bone marrow MSCs into osteoblasts and accelerates the fracture healing process. Furthermore, BMP-2 can also initiate the expression of osteoblast-specific transcription factors such as RUNX2 and activate the transcription and translation of key osteoblast-specific genes like ALP and BGP (Zhang *et al*., 2020). RUNX2, closely related to osteogenesis, is an important osteogenic transcription factor that regulates classic bone metabolism pathways, including BMP/Samd, Notch, and Wnt (Yan *et al*., 2022). VEGF is a specific angiogenesis regulator that acts on endothelial cells, promoting their proliferation and directly or indirectly stimulating angiogenesis. VEGF is also involved in regulating the fracture healing process, and inhibition of VEGF can delay fracture healing (Dong *et al*., 2024). Moreover, VEGF enhances the expression of RUNX2 in bone marrow MSCs and promotes osteoblast formation (Shen *et al*., 2022). It was observed that the expression of BMP-2, RUNX2, and VEGF in the tibia of rats with tibial fractures was increased, and after oral administration of HXHYD, the expression of BMP-2, RUNX2, and VEGF was significantly higher. These results suggest that HXHYD can further activate BMP-2 and RUNX2 expression to induce the differentiation of bone marrow mesenchymal cells, promoting the proliferation of osteoblasts and chondrocytes. Additionally, HXHYD can also stimulate VEGF expression, thereby promoting angiogenesis at the fracture site to ensure an adequate blood and nutrient supply. All these factors contribute to the healing of tibial fractures.

Notch1 is one of the classical receptors in the Notch pathway, which plays a crucial role in regulating the osteogenic differentiation of bone marrow MSCs and influencing bone metabolism. The Notch pathway is an important regulator of the proliferation and differentiation of skeletal cells. Activation of the Notch1 pathway leads to a reduction in cartilage volume and an increase in the mineralization of callus tissue, which promotes fracture repair. Yu *et al*. (2020) found that lncRNA-FTX can target and bind to miR-137, inhibiting the activation of the Notch1 pathway, thereby reducing osteoclastogenesis and inhibiting osteoblastic differentiation (Yu *et al*., 2020). Liu *et al*. (2020) constructed a rabbit tibial fracture model and found that Notch1 protein expression level in the right tibial tissue was markedly inferior to in the parathyroid hormone-treated group (Liu *et al*., 2020). These findings are consistent with our observation that oral administration of HXHYD led to an increase in Notch1 protein relative expression level in the tibial tissue of rats with tibial fractures. Activation of the Notch1 pathway may indirectly regulate the expression of PPARγ by affecting the transcription of specific genes (Awad *et al*., 2024). A decrease in the relative expression level of PPARγ protein in the tibial tissue of rats with tibial fractures was observed.

PPARγ, a key regulator of adipogenesis (Liu *et al.,* 2024), was markedly downregulated (40% reduction in HXHYD group versus controls). This downregulation may facilitate fracture healing through a dual mechanism of action. First, the inhibition of PPARγ can reduce the differentiation of bone marrow MSCs into adipocytes, thereby preserving a larger pool of osteoprogenitor cells (Tang *et al.,* 2023). Inhibition of the PPARγ pathway can also decrease the expression of fatty acid-binding protein 4 (FABP4), which has been shown to suppress bone formation by interfering with insulin signaling (Yang *et al.,* 2024). In this study, the HXHYD group exhibited a 60% increase in ALP activity and a 55% increase in BGP levels, suggesting that PPARγ inhibition may enhance osteoblast mineralization function by improving insulin sensitivity. This finding is consistent with the conclusion of Yang *et al.* (2024), who demonstrated that PPARγ inhibitors significantly increase ALP activity and osteocalcin secretion in fractured rats.

HXHYD group showed a drastic increase in Notch1 protein expression versus positive group, whereas no activation of the Notch1 pathway was observed in positive group. The inhibition of PPARγ protein was more pronounced, suggesting that HXHYD may promote bone repair through dual regulation of Notch1 activation and PPARγ inhibition. These results indicate that, while both HXHYD and Xianling Gubao can promote fracture healing, their molecular mechanisms differ considerably. HXHYD may achieve more efficient bone regeneration and inflammation regulation through the Notch1/PPARγ/CD36 pathway. CD36, a fatty acid transporter receptor, exhibited upregulation (2.2-fold increase in the HXHYD group), which may influence fracture healing by regulating lipid metabolism and inflammatory responses. Recent studies have shown that CD36 can inhibit the release of pro-inflammatory cytokines TNF-α and IL-6 by activating TLR4/NF-κB pathway (Wang and Lu, 2021), which aligns with the 53% reduction in serum TNF-α levels observed in the HXHYD group in our study. Furthermore, CD36-mediated fatty acid uptake may provide energy substrates for osteoblasts, promoting collagen synthesis and matrix mineralization (Wang *et al.,* 2020). Future research should further explore the metabolic reprogramming role of CD36 in bone repair, particularly its interaction with Notch1 pathway.

However, this study also has certain limitations, such as the failure to investigate the effect of HXHYD on the fracture microenvironment in tibial fracture rats, and the lack of clinical trials to verify the efficacy and safety of this decoction in treating tibial fractures.

**Conclusion:** To explore the potential mechanism of HXHYD in treating tibial fractures, a tibial fracture rat model was established in this study. It was found that after gavage with HXHYD, the healing process of tibial fractures was promoted. This effect was primarily achieved by reducing the release of pro-inflammatory cytokines (TNF-α, IL-1β, and IL-6), increasing the expression of osteogenic cytokines (ALP, BGP, and IGF-1), promoting the transcription and translation of related genes (BMP-2, RUNX2, and VEGF), and regulating the Notch1/PPARγ/CD36 pathway. Furthermore, gavage with HXHYD also enhanced the bone biomechanical strength in tibial fracture rats.

**Authors' Contribution:** Fei Zhao and Mian Wang contributed to the study conception and design. Material preparation, data collection, and analysis were performed by Fei Zhao and Mian Wang. The first draft of the manuscript was written by Fei Zhao and Mian Wang, and all authors commented on the previous versions of the manuscript. All authors read and approved the final manuscript.

**Declaration of conflicting interests:** The author(s) declared no potential conflicts of interest with respect to the research, authorship, and/or publication of this article.

**Animal rights statement:** The local Ethics Committee of Xidian Group Hospital (Xi'an, China) had authorized the animal experiment project of this study.

**Funding/Support**: There is no Funding/Support.

## REFERENCES

Awad, K.S., S. Wang, E.J. Dougherty, A. Keshavarz, C.Y. Demirkale, Z.X. Yu, L. Miller, J.M. Elinoff and R.L. Danner (2024). BMPR2 Loss Activates AKT by Disrupting DLL4/NOTCH1 and PPARγ Signaling in Pulmonary Arterial Hypertension. Int J Mol Sci. 25(10):5403. https://doi.org/10.3390/ijms25105403

Coates, B.A., J.A. McKenzie, S. Yoneda and M.J. Silva (2021). Interleukin-6 (IL-6) deficiency enhances intramembranous osteogenesis following stress fracture in mice. Bone. 143:115737. https://doi.org/10.1016/j.bone.2020.115737

Costanzo, G., A. Naselli, M.L. Arpi, T. Piticchio, R. Le Moli, A. Belfiore and F. Frasca (2024). Very low serum IGF-1 levels are associated with vertebral fractures in adult males with beta-thalassemia major. J Endocrinol Invest. 47(7):1691-1700. https://doi.org/10.1007/s40618-023-02270-6

Cruz, J.P., J.B. Michaud, N.L. Van Rysselberghe, D. Walsh, R. Svetgoff, R. Bailey, S.B. Pirkle, M.F. Megerian, G.J. Harbison, J.A. Becerra, B. Sakka, A. Vega, H.L. Bohlen, A. Holloway, A. Finlay, J.A. Scolaro, J.T. Patterson, S.T. Campbell, J. Hebert-Davies, S.J. Warner, L.H. Goodnough, J.A. Bishop and M.J. Gardner

(2024). Outcomes of isolated medial tibial plateau fractures by fracture morphology. Injury. 55(8):111662. https://doi.org/10.1016/j.injury.2024.111662

Dong, R., J. Wei, S. Tian, J. Wang, Y. Ma, Y. Li, R.X. Liu and Y.Q. Liu (2024). Single-cell RNA transcriptomics reveals Du-Zhong-Wan promotes osteoporotic fracture healing via YAP/β-catenin/VEGF axis in BMSCs. Phytomedicine. 135:155572. https://doi.org/10.1016/j.phymed.2024.155572

Hou, Y., X. Li, X. Wang, T. Dong and J. Yang (2022). The effect of Huoxue Huayu decoction on restenosis after percutaneous coronary intervention in patients with coronary heart disease: A protocol for systematic review and meta-analysis. Medicine (Baltimore). 101(4):e28677. https://doi.org/10.1097/MD.0000000000028677

Ling, Y. (2024). Effect of Huoxue Huayu decoction on limb swelling in the late stage of bone injury and its influence on motor function. Pak J Pharm Sci. 37(5):1087-1092. https://doi.org/10.36721/PJPS.2024.37.5.REG.1087-1092.1

Lin, J.Y., H.M. Kuang, K. Rong, L. Peng, J.J. Kuang and X. Yan (2024). Effectiveness of desertliving cistanche in managing hyperlipidemic osteoporosis in ovariectomized rats through the PI3K/AKT signaling pathway. J Orthop Surg Res. 19(1):393. https://doi.org/10.1186/s13018-024-04890-x

Liu, Q.H., L.M. Liao, H. Wu, Y.P. Lin and S. Yu (2020). PTH promotes rabbit tibial fracture healing via the Notch signaling pathway. Eur Rev Med Pharmacol Sci. 24(4):1616-1623. https://doi.org/10.26355/eurrev_202002_20336

Liu, X., M. Zhou, Y. Wu, X. Gao, L. Zhai, L. Liu and H. Geng (2024). Erythropoietin regulates osteoclast formation via up-regulating PPARγ expression. Mol Med. 30(1):151. https://doi.org/10.1186/s10020-024-00931-7

Muwanga, G.P.B, J. Siliezar-Doyle, A.A. Ortiz, J. Kaslow, E.S. Haight and V.L. Tawfik (2022). The Tibial Fracture-Pin Model: A Clinically Relevant Mouse Model of Orthopedic Injury. J Vis Exp. (185):10.3791/63590. https://doi.org/10.3791/63590

Novak, S., E. Roeder, B.P. Sinder, D.J. Adams, C.W. Siebel, D. Grcevic, K.D. Hankenson, B.G. Matthews and I. Kalajzic (2020). Modulation of Notch1 signaling regulates bone fracture healing. J Orthop Res. 38(11):2350-2361. https://doi.org/10.1002/jor.24650

Pai, S.N. and M.M. Kumar (2023). Combination-type periprosthetic tibial fracture: Felix type (II+IV)A. BMJ Case Rep. 16(2):e252464. https://doi.org/10.1136/bcr-2022-252464

Park, J., G. Yan, K.C. Kwon, M. Liu, P.A. Gonnella, S. Yang and H. Daniell (2020). Oral delivery of novel human IGF-1 bioencapsulated in lettuce cells promotes musculoskeletal cell proliferation, differentiation and diabetic fracture healing. Biomaterials. 233:119591. https://doi.org/10.1016/j.biomaterials.2019.119591

Sabaté-Brescó, M., C.M. Berset, S. Zeiter, B. Stanic, K. Thompson, M. Ziegler, R.G. Richards, L. O'Mahony and T.F. Moriarty (2021). Fracture biomechanics influence local and systemic immune responses in a murine fracture-related infection model. Biol Open. 10(9):bio057315. https://doi.org/10.1242/bio.057315

Saito, H., S. Shoji, A. Kuroda, G. Inoue, R. Tazawa, H. Sekiguchi, K. Fukushima, M. Miyagi, M. Takaso and K. Uchida (2023). In situ-formed hyaluronan gel/BMP-2/hydroxyapatite composite promotes bone union in refractory fracture model mice. Biomed Mater Eng. 34(6):537-544. https://doi.org/10.3233/BME-230021

Schumm, A.K., E.A. Craige, N.K. Arora, P.J. Owen, N.L. Mundell, B. Buehring, U. Maus and D.L. Belavy (2023). Does adding exercise or physical activity to pharmacological osteoporosis therapy in patients with increased fracture risk improve bone mineral density and lower fracture risk? A systematic review and meta-analysis. Osteoporos Int. 34(11):1867-1880. https://doi.org/10.1007/s00198-023-06829-0

Shang, L., Y. Wang, J. Li, F. Zhou, K. Xiao, Y. Liu, M. Zhang, S. Wang and S. Yang (2023). Mechanism of Sijunzi Decoction in the treatment of colorectal cancer based on network pharmacology and experimental validation. J Ethnopharmacol. 302(Pt A):115876. https://doi.org/10.1016/j.jep.2022.115876

Shen, Z., W. Dong, Z. Chen, G. Chen, Y. Zhang, Z. Li, H. Lin, H. Chen, M. Huang, Y. Guo and Z. Jiang (2022). Total flavonoids of Rhizoma Drynariae enhances CD31hiEmcnhi vessel formation and subsequent bone regeneration in rat models of distraction osteogenesis by activating PDGF-BB/VEGF/RUNX2/OSX signaling axis. Int J Mol Med. 50(3):112. https://doi.org/10.3892/ijmm.2022.5167

Shimo, T., H. Takebe, T. Okui, Y. Kunisada, S. Ibaragi, K. Obata, N. Kurio, K. Shamsoon, S. Fujii, A. Hosoya, K. Irie, A. Sasaki and M. Iwamoto (2020). Expression and Role of IL-1β Signaling in Chondrocytes Associated with Retinoid Signaling during Fracture Healing. Int J Mol

Sci. 21(7):2365. https://doi.org/10.3390/ijms21072365

Tang, W., Z. Ding, H. Gao, Q. Yan, J. Liu, Y. Han, X. Hou, Z. Liu, L. Chen, D. Yang, G. Ma and H. Cao (2023). Targeting Kindlin-2 in adipocytes increases bone mass through inhibiting FAS/PPARγ/FABP4 signaling in mice. Acta Pharm Sin B. 13(11):4535-4552. https://doi.org/10.1016/j.apsb.2023.07.001

Wang, J., C. Wei, M. Pan, X. Liu and Y. Pan (2020). Effect of Huoxue Huayu decoction on Wnt/β-catenin signal pathway expression in rats with severe traumatic brain injury. Zhonghua Wei Zhong Bing Ji Jiu Yi Xue. 32(9):1101-1106. https://doi.org/10.3760/cma.j.cn121430-20200615-00470

Wang, L., R. Hu, P. Xu, P. Gao, B. Mo, L. Dong and F. Hu (2024). CD90's role in vascularization and healing of rib fractures: insights from Dll4/notch regulation. Inflamm Res. 73(12):2263-2277. https://doi.org/10.1007/s00011-024-01962-w

Wang, T. and H. Lu (2021). Ganoderic acid A inhibits ox-LDL-induced THP-1-derived macrophage inflammation and lipid deposition via Notch1/PPARγ/CD36 signaling. Adv Clin Exp Med. 30(10):1031-1041. https://doi.org/10.17219/acem/137914

Wood, M.J., T. Al-Jabri, A.R. Maniar, T. Stelzhammer, B. Lanting and P.V. Giannoudis (2024). Periprosthetic tibial fracture as a complication of unicompartmental knee arthroplasty: Current insights. Injury. 55(8):111654. https://doi.org/10.1016/j.injury.2024.111654

Yan, C.P., X.K. Wang, K. Jiang, C. Yin, C. Xiang, Y. Wang, C. Pu, L. Chen and Y.L. Li (2022). β-Ecdysterone Enhanced Bone Regeneration Through the BMP-2/SMAD/RUNX2/Osterix Signaling Pathway. Front Cell Dev Biol. 10:883228. https://doi.org/10.3389/fcell.2022.883228

Yang, G., K. Liu, S. Ma and P. Qi (2024). PPARγ inhibition promotes osteogenic differentiation of bone marrow mesenchymal stem cells and fracture healing. J Cell Biochem. 125(6):e30568. https://doi.org/10.1002/jcb.30568

Yong, E.L., W.F. Cheong, Z. Huang, W.P.P. Thu, A. Cazenave-Gassiot, K.Y. Seng and S. Logan (2021). Randomized, double-blind, placebo-controlled trial to examine the safety, pharmacokinetics and effects of Epimedium prenylflavonoids, on bone specific alkaline phosphatase and the osteoclast adaptor protein TRAF6 in post-menopausal women. Phytomedicine. 91:153680. https://doi.org/10.1016/j.phymed.2021.153680

Yu, Y., P. Yao, Z. Wang and W. Xie (2020). Down-regulation of FTX promotes the differentiation of osteoclasts in osteoporosis through the Notch1 signaling pathway by targeting miR-137. BMC Musculoskelet Disord. 21(1):456. https://doi.org/10.1186/s12891-020-03458-0

Zhang, E., S. Miramini, M. Patel, M. Richardson, P. Ebeling and L. Zhang (2022). Role of TNF-α in early-stage fracture healing under normal and diabetic conditions. Comput Methods Programs Biomed. 213:106536. https://doi.org/10.1016/j.cmpb.2021.106536

Zhang, L., G. Jiao, S. Ren, X. Zhang, C. Li, W. Wu, H. Wang, H. Liu, H. Zhou and Y. Chen (2020). Exosomes from bone marrow mesenchymal stem cells enhance fracture healing through the promotion of osteogenesis and angiogenesis in a rat model of nonunion. Stem Cell Res Ther. 11(1):38. https://doi.org/10.1186/s13287-020-1562-9

Zhang, W., F. Yang, Q. Yan, J. Li, X. Zhang, Y. Jiang and J. Dai (2023). Hypoxia inducible factor-1α related mechanism and TCM intervention in process of early fracture healing. Chin Herb Med. 16(1):56-69. https://doi.org/10.1016/j.chmed.2023.09.006

Zhang, Y., X. Fan, K. Pang and D. Liu (2024). The clinical effect of Huoxue Huayu Recipe combined with ibuprofen in patients with postoperative pain after ankle fracture. Biotechnol Genet Eng Rev. 40(3):2613-2627. https://doi.org/10.1080/02648725.2023.2200350

Zheng, C.S., Z.Q. Zhuang, X.J. Xu, J.X. Ye, H.Z. Ye, X.H. Li, G.W. Wu, H.F. Xu and X.X. Liu (2014). In silico search for multi-target therapies for osteoarthritis based on 10 common Huoxue Huayu herbs and potential applications to other diseases. Mol Med Rep. 9(3):857-62. https://doi.org/10.3892/mmr.2014.1914.

Zheng, Y. W., L. F. Wu, Y. H. Zhao, L.H. Wu and J. Li (2020). Network Meta-analysis of Huoxue Huayu Chinese medicine injections on hypertensive nephropathy. Zhongguo Zhong Yao Za Zhi. 45(20):4997-5007. https://doi.org/10.19540/j.cnki.cjcmm.20200322.502

Zhou, L., J. Wang and W. Mu (2023). BMP-2 promotes fracture healing by facilitating osteoblast differentiation and bone defect osteogenesis. Am J Transl Res. 15(12):6751-6759. https://pmc.ncbi.nlm.nih.gov/articles/PMC10767540/.